ORNL-TM-4051

AEROSOL PHYSICS OF ASBESTOS FIBERS: INTERCEPTION

Birney R. Fish

OAK RIDGE NATIONAL LABORATORY
OPERATED BY UNION CARBIDE CORPORATION • FOR THE U.S. ATOMIC ENERGY COMMISSION

ORNL-TM-4051

Contract No. W-7405-eng-26

HEALTH PHYSICS DIVISION

AEROSOL PHYSICS OF ASBESTOS FIBERS: INTERCEPTION

Birney R. Fish*

JULY 1974

*Present address:
Executive Assistant for Energy Resource Management
Kentucky Department for Natural Resources and
Environmental Protection
Frankfort, Kentucky 40601

OAK RIDGE NATIONAL LABORATORY
Oak Ridge, Tennessee 37830
operated by
UNION CARBIDE CORPORATION
for the
U. S. ATOMIC ENERGY COMMISSION

CONTENTS

AEROSOL PHYSICS OF ASBESTOS FIBERS: INTERCEPTION

Birney R. Fish

ABSTRACT

A theoretical analysis of deposition by geometrical interception of elongated fibers is described. Deposition, or penetration, is strongly affected by fiber orientation. No fibers oriented perpendicularly to the flow direction can penetrate a hollow circular cylinder having a diameter (D) smaller than the fiber length (L). In the case of randomly oriented fibers, when $L = D$ the estimated fraction penetrating is nearly 30% and is approximately 27 (D/L)% for $L > 3D$. For the case of fibers having a cosine distribution of position angle relative to the flow direction, penetration is calculated to be 42.4 (D/L)% for $L \geq D$.

INTRODUCTION

Knowledge of the transport and deposition of airborne fibers in the respiratory system, air samplers, and air cleaning devices is a fundamental requirement for solving some of the basic problems associated with the inhalation toxicity of asbestos. Deposition of isometric particles such as spheres, cubes, and other regular polyhedra is governed primarily by sedimentation, inertial impaction, and diffusion and to a lesser extent by geometric interception, adventitious electrical fields, and thermo- and diffusiophoresis. Similar mechanisms are involved in the deposition of long fibrous particles; however, in this case the relative order of significance is entirely different. As indicated by Timbrell,[1] the interception mechanism is far more important than the others in controlling the deposition of asbestos fibers in the lungs.

Any serious attempt to study the inhalation toxicity of asbestos should take into consideration the major significance of interception with respect to the generation and sampling of fibrous aerosols and in connection with their administration to laboratory animals. This paper deals mostly with the mechanism of fiber deposition by geometrical interception and its relevance to the generation, sampling, and inhalation of asbestos fibers.

NATURE OF ASBESTOS FIBERS

Asbestos is a term that applies to a number of different fibrous mineral silicates. While the word is used to describe any mineral that breaks down into fibers, it is most commonly applied to two broad groups--serpentine, represented by chrysotile asbestos, and amphibole, which is subdivided into anthophyllite, amosite, crocidolite, tremolite, and actinolite. Chrysotile is by far the most widely used variety of asbestos, comprising more than 90% of the world's usage.[2] These minerals share the common property that their basic molecular structure consists of units that are linked together much more strongly in one direction than in the others. Depending on the forces applied to a piece of asbestos mineral, the resulting fragments may be individual fibrils, single crystals perhaps 0.01 to 0.8 μm in diameter, or bundles of fibrils large enough to behave as isometric particles. Aerosols associated with occupational exposure to asbestos are commonly found to consist of particles ranging from individual fibers to isometric fragments and various combinations in between, including fluffy aggregates of fibers, fibers having small isometric particles attached to them, and aggregates of isometric particles.[1,3] The individual fibers may be straight and essentially cylindrical, or they may be curled, as seems to be rather common in the case of chrysotile.[4]

Undoubtedly, all of the shapes and forms of asbestos particles have some bearing on the problem of inhalation toxicity; however, the behavior of compact, nearly isometric particles can be interpreted on the basis of conventional models.[5] For the purpose of this report, attention is limited to the interception mechanism of particle deposition, and only two classes of particles will be considered--straight cylindrical fibers of negligible diameter and fluffy aggregates of spherical shape.

INTERCEPTION--PREFERRED ORIENTATION

A fiber oriented perpendicular to the direction of flow through an opening presents its *maximum dimension* to the opening; consequently, the probability of penetration is minimized. In this case it is clear that if the fiber length L exceeds the diameter D of a circular opening, no penetration will occur. For fiber lengths shorter than D and with the fiber perpendicular to the direction of flow, the fraction penetrating a circular opening depends on the position of the fiber at the entry. The geometry of the problem is illustrated in Fig. 1 (a). Because of circular symmetry, fibers of equal length L can be treated as a family of fibers oriented parallel to one another. To see this, construct the diameter perpendicular to the fiber, and, by rotation of the fiber and diameter, the diameter may be made to coincide with the diameter shown in Fig. 1 (b). Thus the model is simplified to the case illustrated in Fig. 1 (b) where all fibers of length L can be treated as if they were parallel to the fiber shown. Clearly any such fiber will contact the wall of the opening if its end lies outside of the cross-hatched area defined by translating the circular arc of the conduit wall a distance L parallel to the fiber.

From Fig. 1 (b) it is clear that

$$y = R - 1/2\ L;$$

thus,

$$\left(1 - \frac{y}{R}\right) = \frac{L}{2R} = \frac{L}{D}$$

and

$$z = \sqrt{2yR - y^2}.$$

The cross-hatched area is

$$A = 2R^2\left\{\left[\cos^{-1}\left(1 - \frac{y}{R}\right)\right] - \left[\left(1 - \frac{y}{R}\right)\sqrt{1 - \left(1 - \frac{y}{R}\right)^2}\right]\right\},$$

and the total area of the opening is πR^2; thus the ratio to the total area of the area available as location for the endpoint of a fiber penetrating is taken to be

$$F = \frac{2}{\pi}\left[\cos^{-1}\left(\frac{L}{D}\right) - \frac{L}{D}\sqrt{1 - \left(\frac{L}{D}\right)^2}\right]. \qquad (1)$$

ORNL-DWG 72-13443

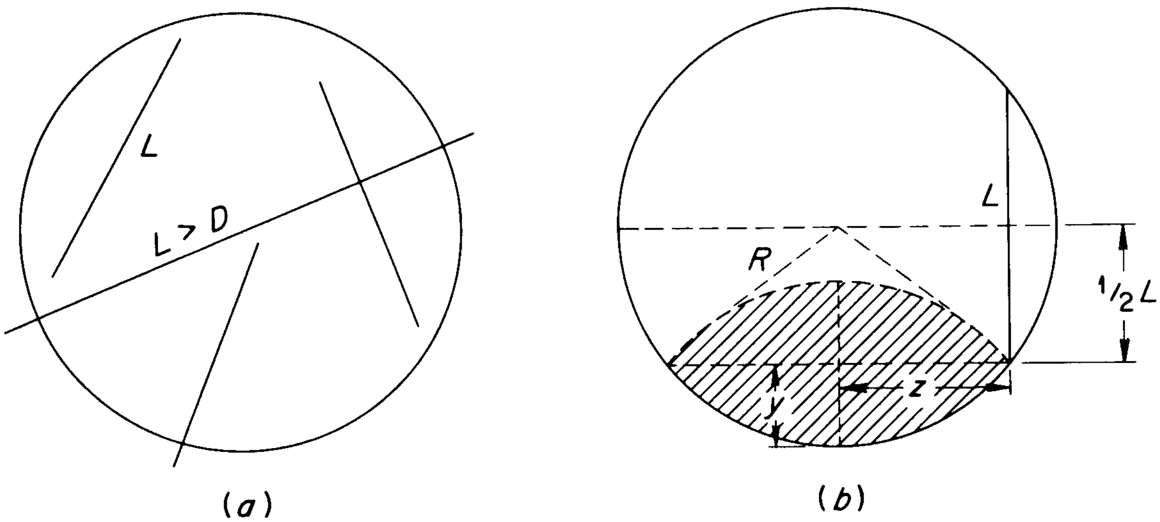

Fig. 1. Schematic Model for the Penetration of a Fiber Through a Circular Opening.

ORNL-DWG 72-13444

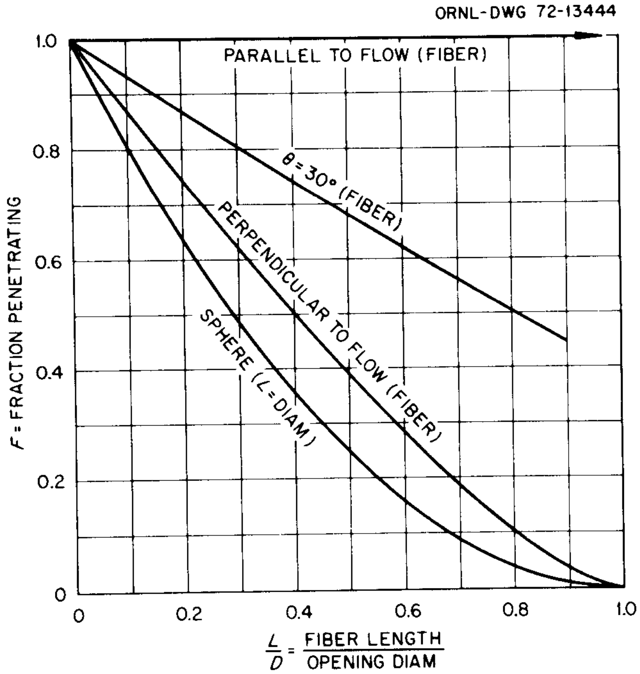

Fig. 2. Fraction of Fibers (and spheres) Penetrating a Circular Opening as a Function of Orientation and of $\frac{L}{D}$ (or $\frac{d}{D}$ for spheres).

This assumes the endpoints of such fibers are randomly distributed in space, and F represents the probability that the fiber has an endpoint in the cross-hatched area.

Fibers oriented parallel with the flow through a circular opening present their minimum dimension for capture. If the fiber diameter is taken to be very small compared with the diameter of the opening, deposition by geometrical interception will also be small for fibers so oriented, and hence penetration will be nearly 100% for all fiber lengths. The expected penetration fractions for the two extremes of orientation are presented in Fig. 2 and in Table 1.

Penetration curves for intermediate orientations can be constructed from the curve for fibers perpendicular to the flow. Thus, for a fiber of length L' making an angle θ with the flow direction, the effective perpendicular length is

$$L = L' \sin \theta .$$

As an example, fibers oriented at 30° from the flow direction present an effective length $L = L' \sin 30° = 1/2\, L'$ in the plane of the opening; thus when the actual L'/D ratio is 1.0, the effective ratio for penetration is 0.5 for which $F = 0.391$. By this means, the penetration curve can be computed for $\theta = 30°$ (Fig. 2) and other orientations.

For comparison, the penetration curve for a sphere of diameter L passing a circular opening of diameter D is given by

$$F = 1 - 2\frac{L}{D} + \left(\frac{L}{D}\right)^2 . \qquad (2)$$

This function is shown in Fig. 2 as a dashed line. Numerical values are included in Table 1.

INTERCEPTION--RANDOM ORIENTATION

For the case of a fiber oriented at a random angle θ from the flow direction, it can be seen by an extension of the treatment in the previous section

Table 1. Calculated Fraction of Spherical Aggregates and Cylindrical Fibers Penetrating a Circular Opening as a Function of Aspect Ratio and Orientation

Aspect Ratio (L/D)	Fraction Penetrating			
	Spherical Aggregates*	Fiber orientation relative to flow direction		
		Perpendicular	Random	Cosine
0.05	0.903	0.936	0.966	0.968
0.1	0.81	0.873	0.926	0.936
0.2	0.64	0.747	0.846	0.873
0.3	0.49	0.624	0.767	0.810
0.4	0.36	0.505	0.690	0.749
0.5	0.25	0.391	0.614	0.688
0.6	0.16	0.285	0.542	0.630
0.7	0.09	0.188	0.474	0.573
0.8	0.04	0.104	0.410	0.520
0.9	0.01	0.037	0.352	0.470
1.0	0	0	0.297	0.424
1.5	0	0	0.186	0.283
2.0	0	0	0.138	0.212
3.0	0	0	0.0908	0.141
5.0	0	0	0.0543	0.0849
10.0	0	0	0.0270	0.0424
20.0	0	0	0.0135	0.0212

*Aspect ratio is defined as sphere diam./diam. of opening.

that the penetration fraction is

$$F(\theta) = \frac{2}{\pi}\left\{\left[\cos^{-1}\left(\frac{L}{D}\sin\theta\right)\right] - \left[\left(\frac{L}{D}\sin\theta\right)\sqrt{1-\left(\frac{L}{D}\sin\theta\right)^2}\right]\right\}. \qquad (3)$$

If all orientations between 0 and $\pi/2$ (radians) are equally likely, the probability of the orientation being within $d\theta$ of θ is

$$P(\theta)\,d\theta = \frac{2}{\pi}\,d\theta,$$

and the expectation value of the penetration fraction (mean penetration fraction) is given by

$$\langle F\rangle = \int_0^{\varphi} \frac{2}{\pi} F(\theta)\,d\theta, \qquad (4)$$

where

$$\varphi = \arcsin\left[\min\left(1, \frac{D}{L}\right)\right].$$

Note that the upper integration limit is the angle for which $L/D \sin\theta = 1$ if $L/D \geq 1$. While $F(\theta)$ cannot readily be integrated in closed form, a numerical integration was performed using Simpson's rule and breaking the interval 0 to $\pi/2$ into 50 increments. The results are given in Fig. 3 and Table 1.

It can be shown that for large aspect ratios (i.e., $L/D >> 1$), the fraction penetrating approaches

$$\langle F\rangle = \frac{8}{3\pi^2}\,\frac{D}{L}. \qquad (5)$$

ORIENTATION IN LAMINAR-CONDUIT FLOW

As pointed out by Fuchs,[6] an elongated particle tends to rotate in a region of shear flow in such a way that the major axis of an ellipsoidal particle is directed near the direction of flow most of the time. This would suggest a mechanism for producing a preferred para-axial orientation for fibers in the shear flow experienced in portions of the respiratory airways and in sampling equipment. The rate of rotation of a prolate ellipsoid in a velocity gradient Γ, approximating a fiber of diameter d and length L, can be shown[6-8] to be

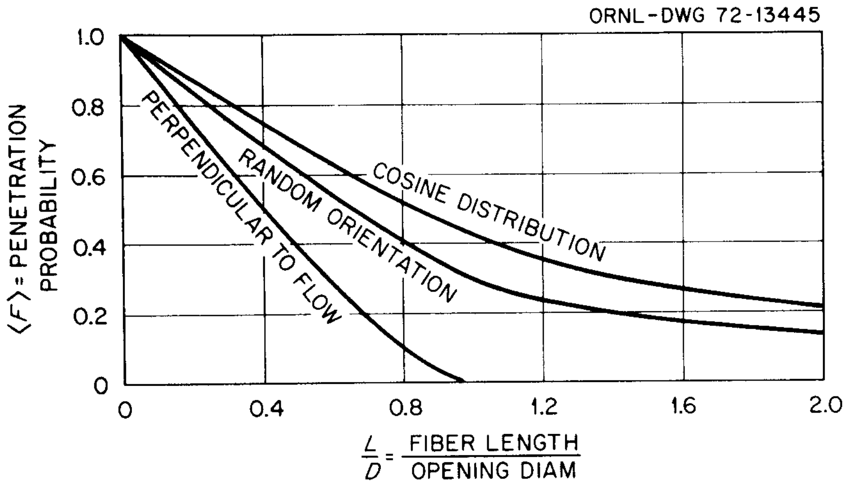

Fig. 3. Penetration Probability of a Fiber through a Circular Opening as a Function of Aspect Ratio and Orientation with Respect to the Flow Direction.

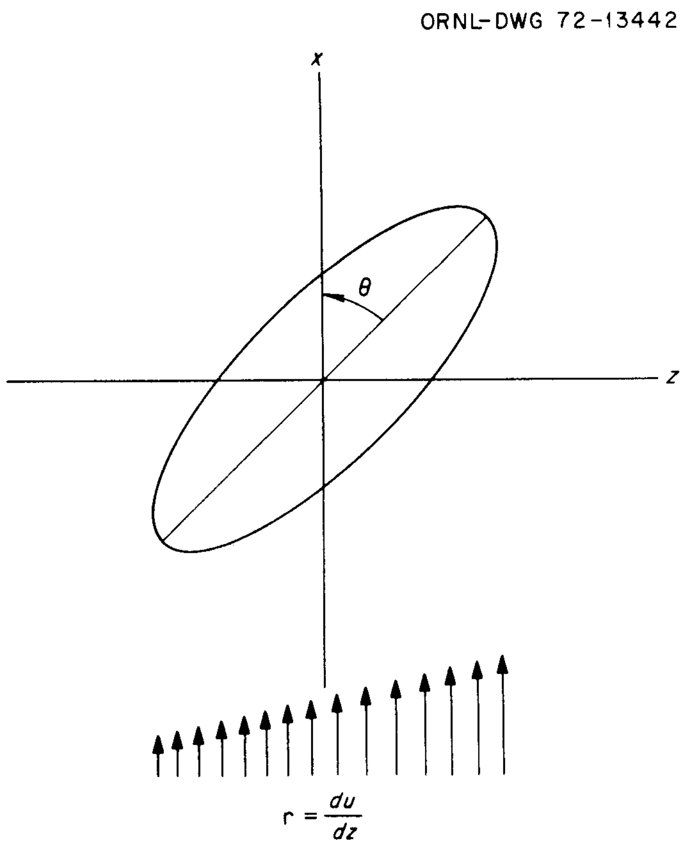

Fig. 4. Rotation of an Ellipsoid in Shear Flow.

$$\frac{d\theta}{dt} = -\Gamma\left(\frac{L^2\sin^2\theta + d^2\cos^2\theta}{L^2 + d^2}\right) \qquad (6)$$

where θ is the angle between the long axis of the fiber and the flow direction (Fig. 4). For a constant velocity gradient, (6) can be integrated to determine the time T required for the fiber to rotate from an orientation perpendicular to the flow to one parallel to the flow; thus,

$$T = \frac{L^2 + d^2}{\Gamma}\int_0^{\frac{\pi}{2}} \frac{d\theta}{L^2\sin^2\theta + d^2\cos^2\theta} = \frac{L^2 + d^2}{\Gamma}\left(\frac{\pi}{2Ld}\right),$$

and for the case $L/d \gg d/L$,

$$T \approx \frac{\pi}{2\Gamma}\left(\frac{L}{d}\right). \qquad (7)$$

Three conclusions related to orientation of fibers can be derived from Eqs. (6) and (7). On a time average basis, fibers in shear flow tend to become aligned with the flow direction, and the approach to an equilibrium alignment is time dependent, going faster for short fibers than for fibers having a high aspect ratio (L/d). The latter conclusion may be at variance with experimental results reported by Timbrell[(1)] for the orientation of glass, amosite, chrysotile, and crocidolite fibers deposited in an aerosol spectrometer. Timbrell observed no significant orientation of fibers having an aspect ratio less than 5 but a rather clear indication of a near-axis preference for those having an aspect ratio greater than 5. However, since no indication was given concerning the rate of shear in the spectrometer nor of transit time to the point (or points) of deposition, the significance of these observations is not clear.

In either case internal shear flow, as in laminar conduit flow, can be expected to produce some degree of alignment of fibers with the flow direction. Two considerations support the use of a cosine probability distribution of angles, that is, that the probability that a fiber will lie within $d\theta$ of θ from the direction of flow is

$$P(\theta)d\theta = \cos\theta d\theta. \qquad (8)$$

This is not far out of line with Timbrell's experimental findings. The fraction of the total fibers expected to lie in the interval from 0 to 30°, 30° to 60°, and 60° to 90° can be calculated from the integral of (8) between these angles for comparison with Timbrell's values (Table 2). Another attractive, although

Table 2. Comparison of Alignment Angle of Chrysotile Asbestos Fibers Observed by Timbrell with that Predicted by the Cosine Distribution Function

Sector (angle with forward direction)	Fraction of Fibers in Sector	
	Timbrell's Data*	Cosine Distribution
0 to 30°	0.45	0.50
30° to 60°	0.30	0.37
60° to 90°	0.25	0.13

not very persuasive, argument in favor of the cosine distribution function (Eq. 8) is that it makes Eq. (3) easily integrable; thus the expectation value of the penetration probability is

$$\langle F\rangle = \frac{2}{\pi}\left\{\int_0^{\varphi}\left[\cos^{-1}\left(\frac{L}{D}\sin\theta\right)\cos\theta d\theta\right] - \int_0^{\varphi}\left(\frac{L}{D}\sin\theta\right)\sqrt{1-\left(\frac{L}{D}\sin\theta\right)^2}\,(\cos\theta d\theta)\right\},$$

where $\varphi = \arcsin\left[\min(1, D/L)\right]$, but this is in the form

$$\langle F\rangle = \frac{2D}{\pi L}\left\{\int_0^{\xi}\cos^{-1}x\ dx - \int_0^{\xi} x\sqrt{1-x^2}\,dx\right\}, \qquad (9)$$

where $\xi = \min(1, L/D)$, for which the solution is

$$\langle F\rangle = \frac{2}{3\pi\left(\frac{L}{D}\right)}\left\{2 + 3\frac{L}{D}\cos^{-1}\frac{L}{D} - \sqrt{1-\left(\frac{L}{D}\right)^2}\left[2+\left(\frac{L}{D}\right)^2\right]\right\}, \qquad (10)$$

(valid in the range $L/D \le 1$).

When $L/D = 1$ in Eq. (10), $\langle F\rangle = 4/3\pi$. For the range $L/D > 1$, the upper integration limit of (9) is 1 and the result is

$$\langle F \rangle = \frac{4}{3\pi}\left(\frac{D}{L}\right), \quad \text{(for } L/D > 1\text{)}. \tag{11}$$

The penetration probabilities for fibers having a cosine distribution of alignment angle, calculated from (10) and (11), are presented in Fig. 3 and in Table 1.

CONCLUSIONS

The results of calculating the fraction of fibers penetrating a circular opening are summarized in Table 1. These numbers give some insight into the question of how fibers as long as 200 μm, found in the alveoli of the lungs,[9] have a finite probability of penetrating respiratory airways that are of the same order of diameter as the length of the fiber. Clearly, the fraction penetrating is severely reduced if the fiber is oriented perpendicularly to the flow direction; nevertheless, because of the assumption of negligible fiber diameter, penetration is expected to be greater for a single fiber than for a spherical aggregate having a diameter the same as the fiber length.

It has been suggested by Timbrell[4] that curly fibers tend to be oriented more randomly with respect to flow than are cylindrical fibers. It is not clear how one should go about describing objectively the shape of curled fibers; however, as a first approximation, perhaps the total length along the fiber can be treated as the appropriate length and penetration estimated on the basis of random orientation. Alternatively, one might take the curled fiber to approximate a prolate ellipsoid having major and minor dimensions the same as the fiber envelope.

As matters stand, it is possible to do a theoretical analysis of deposition by geometrical interception for the two idealized shapes represented by the sphere and the cylinder. There even seem to be real particles that approximate these idealized shapes. However, the many odd-shaped fibers and aggregates defy adequate description, and their behavior is not well understood. The situation is not unlike the case of dealing with the inertial properties of odd (and mixed) shape, size, and density particles. The solution has been to define an inertial parameter, the aerodynamic equivalent size, and to design sampling equipment, such as the cascade impactor,[10,11] yielding results that can be expressed in terms of the aerodynamic equivalent spherical diameter. Similarly, it is suggested that odd-shaped fibers and aggregates may be described in terms of an interception equivalent length. In this connection, a cascade interceptor sampler may be designed to yield results that are expressible in terms of an equivalent length distribution function. Thus, to characterize the respirability of an asbestos aerosol containing compact particles as well as elongated fibers, it may be necessary to perform parallel measurements to determine both the aerodynamic equivalent size distribution and the distribution function for interception equivalent length.

Descriptions of the aerosol generation equipment used in asbestos inhalation research frequently include references to an air elutriation step wherein the upward component of air velocity is held to a constant value. Such a stage is used when dealing with compact particles to effect an aerodynamic separation of sizes for particles having settling velocities greater than, versus those settling slower than, the given upward directed air velocity. It is not uncommon for persons outside the specialized field of aerosol physics to assume that this air elutriation stage is similarly capable of separating fibers according to length. However, because the inertial properties of long fibers depend almost exclusively on their diameters, little, if any, separation on the basis of length is produced in an air elutriator. The real function of such a stage is to separate the small-diameter fibers of various lengths from most of the large compact bundles and from other more nearly isometric particles. It should be clear that control over fiber length requires attention to factors other than inertial parameters. Where control of initial fiber length is feasible, as, for example, in the case of fibers cut on a microtome, air elutriation is a desirable means of eliminating thick bundles of fibers from the high-aspect-ratio single fibers and small-diameter bundles. For sources of fibers containing an irregular distribution of lengths, some control over fiber length may be realized by passing the aerosol through a cascade interceptor; the effluent fibers from a given stage can be expected to have lengths predominantly shorter than a value characteristic of the stage. If the objective is to use fibers shorter than a given size, the effluent from a cascade interceptor can be used directly; alternatively, the fibers collected on each stage can be redispersed to produce an aerosol having a relatively narrow distribution of fiber lengths.

REFERENCES

1. V. Timbrell, "An Aerosol Spectrometer and Its Applications," Chap. 15, pp. 290-330, in Assessment of Airborne Particles (C. C. Thomas, Springfield, 1972), edited by T. T. Mercer, P. E. Morrow and W. Stöber.

2. Richard Gaze, "The Physical and Molecular Structure of Asbestos," Ann. N. Y. Acad. Sci. 132, 23-30 (1965).

3. Morton Corn, documented discussion of ref. 9, p. 443, in Assessment of Airborne Particles (C. C. Thomas, Springfield, 1972), edited by T. T. Mercer, P. E. Morrow and W. Stöber.

4. V. Timbrell, "The Inhalation of Fibrous Dusts," Ann. N. Y. Acad. Sci. 132, 255-273 (1965).

5. P. E. Morrow et al., "Deposition and Retention Models for Internal Dosimetry of the Human Respiratory Tract," Health Phys. 12, 173-207 (1966).

6. N. A. Fuchs, The Mechanics of Aerosols (Pergamon Press, Oxford, 1964).

7. G. B. Jeffery, "The Motion of Ellipsoidal Particles Immersed in a Viscous Fluid," Proc. Roy. Soc. 102A, 161-179 (1923).

8. A. Peterlin and H. A. Stuart, "Zur Theorie der Stromungsdoppelbrechung von Kolloiden und Grossen Molekulen in Losung," Z. Physik 112, 1-19 (1939).

9. V. Timbrell, "Inhalation and Biological Effects of Asbestos," Chap. 22, pp. 429-441, in Assessment of Airborne Particles (C. C. Thomas, Springfield, 1972), edited by T. T. Mercer, P. E. Morrow and W. Stöber.

10. T. T. Mercer, "Aerosol Production and Characterization: Some Considerations for Improving Correlation of Field and Laboratory Derived Data," in Hanford Symposium on Inhaled Radioactive Particles and Gases [Health Phys. 10, 873-887 (1964)].

11. J. O. Ledbetter and B. R. Fish, "The Jet Filter--A Single Stage Size-Selective Sampler for Airborne Particulates," AIHAJ 33, 90-93 (1972).

ORNL-TM-4051

INTERNAL DISTRIBUTION

1. J. A. Auxier
2. T. J. Burnett
3. T. G. Clark
4. K. E. Cowser
5-34. B. R. Fish
35. A. P. Malinauskas
36. C. D. Scott
37. J. L. Scott
38. R. L. Shipp, Jr.
39. W. S. Snyder
40. D. G. Thomas
41. W. A. Thomas
42. J. R. Totter
43. R. L. Walker
44. Nuclear Safety Information Center
45-46. Central Research Library
47. Document Research Library
48-49. Laboratory Records Department
50. Laboratory Records, ORNL R.C.
51. ORNL Patent Office

EXTERNAL DISTRIBUTION

52. Jack L. Durham, Environmental Protection Agency, Technical Center, Research Triangle Park, N. C. 27711.
53. James E. Funk, Dean, College of Engineering, University of Kentucky, Lexington, KY 40506.
54. George Hidy, Science Center, Rockwell International, 1049 Camino dos Rios, Thousand Oaks, CA 91360.
55. Koichi Iinoya, Department of Chemical Engineering, Kyoto University, Sakyo-ku, Kyoto, Japan.
56. J. O. Ledbetter, Department of Civil Engineering, University of Texas, Austin, TX 78712.
57. M. J. Matteson, Chemical Engineering Department, Georgia Institute of Technology, Atlanta, GA 30332.
58. W. J. Megaw, Department of Physics, York University, 4700 Keele Street, Downsview 463, Ontario, Canada.
59. K. Z. Morgan, School of Nuclear Engineering, Georgia Institute of Technology, Atlanta, GA 30332.
60. Robert E. Nickel, Office Planning & Research, Department of Natural Resources & Environmental Protection, Frankfort, KY 40601.
61. Kenneth Noll, Department of Civil Engineering, University of Tennessee, Perkins Hall, Knoxville, TN 37916.
62. Toshiichi Okita, RB 306, Akabane-dai 2-2, Kita-ku, Tokyo, Japan.
63. Clyde Orr, Chemical Engineering Department, Georgia Institute of Technology, Atlanta, GA 30332.
64. Harry C. Saxe, Dean, Speed Scientific School, University of Louisville, Louisville, KY 40208.
65. W. T. Snyder, Department of Engineering Mechanics, University of Tennessee, Knoxville, TN 37916.
66. Carl O. Thomas, Environmental Systems Corporation, McGhee Tyson Airport, Knoxville, TN 37920.

67. Vernon Timbrell, University of Cardiff, Cardiff, Glamorganshire, Wales, Great Britain.
68. Jack Wagman, Environmental Protection Agency, Technical Center, Research Triangle Park, NC 27711.
69. W. H. Wilkie, Tennessee Valley Authority, Muscle Shoals, AL 35660.
70. W. E. Wilson, Environmental Protection Agency, Technical Center, Research Triangle Park, NC 27711.
71. Research and Technical Support Division, U. S. Atomic Energy Commission, Oak Ridge, TN 37830.
72- Technical Information Center, U. S. Atomic Energy Commission, Oak Ridge,
73. TN 37830.